Strict Feedback Nonlinear System Dynamic Surface Asymmetric Prescribed Performance Control

Xinen Liu, Qiang Qu, *Member*, *IAENG,* and Hui Liu

***Abstract*—For a class of strict feedback nonlinear systems with prescribed performance control, a control method based on an asymmetric prescribed performance function is proposed. Traditional prescribed performance functions with symmetric structures generate constraint intervals that are excessively wide during the initial control phase, failing to effectively regulate the fluctuations of tracking errors. To address this problem, a novel prescribed performance function with an asymmetric structure and strip shaped constrained space is introduced. Based on this performance function and the backstepping method integrated with dynamic surface control, a novel prescribed performance controller is designed. The stability of the closed loop system is analyzed via the Lyapunov stability criterion, and the effectiveness of the proposed algorithm is validated through simulations. Compared with existing approaches, the designed controller ensures that the initial value of tracking error falls within the constraint range specified by the prescribed performance function, reduces tracking error fluctuations, improves the transient performance of the system, and guarantees that the tracking error converges to a small neighborhood of the equilibrium point within any predefined time.**

***Index Terms*—Prescribed performance control, asymmetric, dynamic surface control, strictly feedback.**

I. INTRODUCTION

Prescribed performance control (PPC) can ensure both transient and steady state performance of the system, therefore, PPC has attracted the attention of researchers since its proposal [1, 2].

In [3], Y. B. Jiang *et al*. proposed a novel distributed fault tolerant controller to address the finite time consensus problem for multiple Lagrangian systems with actuator faults and prescribed performance. This controller not only ensures the steady state performance of the system but also guarantees its transient performance. The controller enables the errors to converge to a small neighborhood near the equilibrium point within a finite time while maintaining them within the prescribed performance bounds throughout the process. J. Wu *et al*. investigated adaptive optimal fuzzy control for uncertain nonlinear systems with prescribed tracking accuracy. Compared with existing optimal backstepping control methods, the proposed approach constructs the target controller utilizing two C^n class functions, which ensures that the tracking error converges to a prespecified bounded range in [4].

When the prescribed performance function is a constant, it can indeed constrain the output, but the lack for decay property limits its applicability to some extent. To address this issue, researchers have proposed prescribed performance functions with monotonically decaying forms and designed prescribed performance controllers based on these functions. The designed controllers not only ensure the steady state performance of the system but also enhance its transient performance.

In [5], Y. S. Hu *et al*. investigated the practical predefined time fault tolerant control (FTC) problem for uncertain Euler Lagrange systems subject to input saturation and performance constraints. By employing error transformation techniques and velocity functions, the proposed approach guarantees that the tracking error converges within a predefined time while maintaining its overshoot within prescribed performance bounds. To ensure the safety and stability of unmanned surface vehicles during navigation, performance constraints were imposed on the path following control system, significantly enhancing the transient performance of the controller in [6]. Y. N. Yang *et al*. proposed a novel prescribed performance synchronous control scheme for a class of mobile manipulator teleoperation systems with time varying delays and nonholonomic constraints in [7]. In [8], X. Li *et al*. developed a novel prescribed performance controller for maximum power point tracking control in wind power generation systems. This technology allows for the setting of convergence speed and tracking accuracy. D. G. Chu *et al*. proposed a prescribed performance adaptive neural network control method based on funnel control for a single link robotic arm system with quantized input. Unlike traditional funnel control schemes, this method constructs a novel performance function to ensure that the system achieves predefined performance metrics within a predetermined time in [9]. In [10], Y. L. Huang *et al*. addressed the prescribed performance tracking control problem for intelligent vehicle steering systems with inherent model nonlinearities and parametric uncertainties. It developed a novel prescribed performance controller for steer by wire systems by innovatively integrating barrier Lyapunov function techniques.

With the development of prescribed performance functions,

Manuscript received April 9, 2025; revised July 10, 2025.

This work is supported by the Basic Research Project of Liaoning Provincial Department of Education (LJKMZ20220655 and LJ232410146053) and National Natural Science Foundation of China (U21A20483).

Xinen Liu is a PhD student at the School of Electronic and Information Engineering, University of Science and Technology Liaoning, Anshan, Liaoning, 114051, China (e-mail: 221081100045@stu.ustl.edu.cn).

Qiang Qu is a professor at the School of Electronic and Information Engineering, University of Science and Technology Liaoning, Anshan, Liaoning, 114051, China (*corresponding author to provide e-mail: quqiang@ustl.edu.cn).

Hui Liu is a PhD student at the School of Electronic and Information Engineering, University of Science and Technology Liaoning, Anshan, Liaoning, 114051, China (e-mail: 18741273790@163.com).

exponential type prescribed performance functions have gradually gained widespread application in various fields such as state constraints, tracking, and spacecraft position and attitude adjustment. In [11], K. X. Lu *et al*. investigated the adaptive neural network based prescribed performance tracking control problem for the non-strict feedback time delay systems subject with full state constraints. X. N. Xia *et al*. developed a hyperbolic tangent function based prescribed performance tracking control scheme for a class of non-strict feedback nonlinear systems with input time delays and dynamic uncertainties in [12]. In [13], G. Q. Duan *et al*. developed an adaptive prescribed performance controller based on the fully actuated system approach for the attitude and position control of composite spacecraft formations. X. L. Zhang *et al*. developed a fixed time control method based on variable exponential coefficients to enhance both transient and steady state performance of exoskeleton systems in [14].

To further reduce the constraint space determined by the prescribed performance function. Based on the barrier Lyapunov function (BLF) with transformed errors and the finite time prescribed performance function (FTPPF) with arbitrarily setting time, a backstepping based attitude controller was derived, ensuring both transient and steady state performance in [15]. F. Liu *et al*. proposed a fixed time prescribed performance adaptive control method to address the multivariable robust control problem in turbofan engines. Literature [16] introduced a fixed time prescribed performance function (FTPPF) to strictly guarantee both transient performance and steady state accuracy of the control system. In [17], L. P. Xin *et al*. proposed an adaptive fuzzy backstepping control method based on dynamic surface control for the system of cascaded continuous stirred tank reactors. The proposed controller ensures the internal stability of the closed loop system and allows the output signals to asymptotically track their desired signals. In [18], G. Luo *et al*. addressed the problem of autonomous vehicles subject to time varying external disturbances and uncertain nonlinearities, developed a prescribed performance function (PPF) with fixed time convergence properties to construct a feedback controller. A. Q. Wang addressed the trajectory tracking problem for quadrotor UAVs in the presence of modeling errors and external disturbances. A dual loop control system was designed, where the outer position loop employs a prescribed performance adaptive PID algorithm [19].

To impose different constraints on the upper and lower bounds of the tracking error, researchers have further proposed dual function type prescribed performance functions. These functions allow independent control over the upper and lower bounds of the tracking error, providing greater flexibility. It is particularly beneficial in applications where asymmetric error constraints are required, such as in CCSTR, robotics, aerospace systems and so on. In [20], H. X. Ma *et al*. proposed a dual function prescribed performance function by integrating conventional prescribed performance techniques with boundary protection algorithms. However, this performance function exhibits two main limitations: it cannot guarantee finite time convergence of tracking errors, and still uses a symmetric structural constraint. Z. Y. Gao *et al*. developed a finite time dual performance constraint function to construct the prescribed performance controller, which achieves two significant improvements: effective reduction of constraint space, and enhanced control performance in [21].

Whether it is the constant type prescribed performance function [3, 4], the monotonically decaying performance constraint function [5, 6, 13, 14], the improved monotonically decaying performance constraint function [18, 19], or the dual function type prescribed performance function [20, 21], all of them can achieve the goal of improving the transient performance of the system while ensuring its steady state performance. However, the prescribed performance functions still have the following shortcomings: Firstly, the constraint space formed by these prescribed performance functions in the initial stage is relatively large, failing to effectively control the fluctuations of the system's tracking error. Secondly, the above prescribed performance control methods all require the assumption that the initial value of the tracking error is within the constraint range; otherwise, it may cause system instability.

To further improve the transient performance of strict feedback nonlinear systems and reduce the fluctuations of tracking errors during the initial phase of control, this paper proposes an asymmetric prescribed performance function (APPF) and designs an asymmetric prescribed performance controller (APPC) by combining dynamic surface control and the backstepping method. Compared with existing research, the contributions of this paper are as follows:

(1) The proposed asymmetric prescribed performance function is composed of two different constraint functions, where one function serves as the upper bound of the constraint space, and the other serves as the lower bound. Unlike the traditional prescribed performance functions in [11, 12], whose constraint space are constructed adopting the original constraint function and its opposite function, this paper uses two distinct prescribed functions to form the constraint space. This approach results in a more flexible constraint space, smaller tracking error fluctuations, and faster convergence speed.

(2) The proposed asymmetric prescribed performance function considers the influence of the initial tracking error and incorporates it as a parameter of the prescribed performance function. This ensures that the initial value of tracking error falls within the constraint range, thereby eliminating the assumption in traditional prescribed performance control that the initial value of tracking error must already lie within the constraint range.

(3) Other than prescribed performance functions in [11, 13, 16] which are asymptotic convergence and whose convergence time are theoretically infinite, the prescribed performance function proposed in this paper can achieve convergence in finite time and owns a faster convergence speed.

(4) Rather than commanded filtering technique used in [23], the first-order dynamic surface technique [22] is used to estimate the derivative of the virtual control signal, which solve the “differential explosion” problem in backstepping method and reduce the computational complexity at the same time.

II. Problem Formulation Preliminaries

Consider the following strict feedback nonlinear system.

where $x_i(t)\,(i=1,2,...,n)$, $u(t)\in\mathbb{R}$, $y(t)\in\mathbb{R}$ being system state variables, input variables, and output variables respectively; $f_i(\cdot)$ and $g_i(\cdot)$ being known smooth functions,

$g_i(\cdot) \neq 0$, $\bar{x}_i(t) = [x_1(t), x_2(t), ..., x_i(t)]^{\mathrm{T}}$. For the convenience, all time variables t is omitted below.

$$\begin{cases} \dot{x}_1(t) = f_1(\bar{x}_1(t)) + g_1(\bar{x}_1(t))x_2(t), \\ \dot{x}_i(t) = f_i(\bar{x}_i(t)) + g_i(\bar{x}_i(t))x_{i+1}(t), \\ \dot{x}_n(t) = f_n(\bar{x}_n(t)) + g_n(\bar{x}_n(t))u(t), \\ y = x_1, \end{cases} \tag{1}$$

Assumption 1 [24]: The desired signal is continuous, bounded, and *n* orders differentiable.

The control objectives of this paper are as follows:

For a class of strict feedback nonlinear systems (1), based on the proposed finite time asymmetric prescribed performance function, an asymmetric prescribed performance controller is designed to achieve the following goals:

(1) The system output can track the desired signal within a finite time, and the closed loop system is uniformly bounded and stable. The tracking error of the system converges to a small neighborhood near the equilibrium point.

(2) The tracking error of the system satisfies the transient and steady performance predefined by the asymmetric prescribed performance function.

Lemma 1 (Lyapunov Stability [17]): Consider a nonlinear system $\dot{x}(t) = f(\bar{x}(t))$, where $x(t)$ representing the state, $f(\cdot)$ representing nonlinear smooth functions, if there exists a positive definite continuous function $V(x(t))$ satisfying the following inequality:

$$\dot{V}(x(t)) \leq -aV + b, \tag{2}$$

where $a > 0$ and $b > 0$, then the system is uniformly ultimately bounded stable.

Lemma 2 [25]: For $\rho > |z_1|, z_1 \in R$, there exists

$$\log\left(\frac{\rho^2}{\rho^2 - z_1^2}\right) \leq \frac{z_1^2}{\rho^2 - z_1^2}. \tag{3}$$

Lemma 3 [26][27]: For $\forall a, b \in R$, $L_i > 0$, there exists

$$ab \leq \frac{1}{2L_i^2}a^2 + \frac{L_i^2}{2}b^2. \tag{4}$$

To achieve control objective (2), the tracking error is constrained as follows:

$$b(t) < e(t) < a(t), t \geq 0, \tag{5}$$

where $e(t) = y(t) - y_r(t)$, $y(t)$ and $y_r(t)$ are the output and the desired signal of the system.

e_0 is the initial value of the tracking error; $a_0 > 0$ and $b_0 > 0$ are design parameters representing the deviation degree of the upper and lower bounds of the constraint space from the initial tracking error at the initial time, respectively. $a_\infty > 0$ and $b_\infty > 0$ are design parameters representing the upper and lower bounds of the steady state tracking error of the system, respectively, $a_0 > a_\infty$ and $b_0 > b_\infty$.

From (6) and (7), it can be seen that the prescribed performance function proposed in this paper differs from those in [11,12]. It introduces the initial value of tracking error e_0 in the proposed prescribed function ensuring that the initial value of the tracking error falls within the constraint space. This effectively overcomes the assumption in traditional prescribed performance control that the initial value of tracking error must lie in the constraint space, facilitates practical application of prescribed performance.

$$a(t) = \begin{cases} e_0 + a_0 - a_\infty \left(1 - \frac{t}{T}\right)^{n+1} + a_\infty, \\ \qquad\qquad 0 \leq t < T, \\ a_\infty, \qquad\qquad t \geq T, \end{cases} \tag{6}$$

$$b(t) = \begin{cases} e_0 - b_0 + b_\infty \left(1 - \frac{t}{T}\right)^{n+1} - b_\infty, \\ \qquad\qquad 0 \leq t < T, \\ -b_\infty, \qquad\qquad t \geq T, \end{cases} \tag{7}$$

Depending on the relative magnitudes of e_0 , $a_0 - a_\infty$ and $b_0 - b_\infty$, the following four types of constraint spaces may be formed:

Case 1: An asymmetric strip shaped constraint space.

When $e_0 \in [b_0 - b_\infty, \infty)$, the constraint space formed by (6) and (7) is shown in Fig. 1. As can be seen from Fig. 1, this constraint space has an asymmetric structure, which is different from the symmetric structure in [11, 12] formed by the original performance function and its form of opposite function.

The asymmetric strip shaped constraint space proposed in this paper is composed of two different constraint functions, where $a(t)$ serves as the upper boundary of the constraint space, $b(t)$ serves as the lower boundary. The initial values of the constraint functions $a(t)$ and $b(t)$ are both greater than or equal to 0 and lie on the upper side of $-b_\infty$. The initial range of the constraint space is $[e_0 - b_0, e_0 + a_0]$ to ensure the initial value of the tracking error e_0 falls within the constraint range.

Case 2: An approximately symmetric trumpet shaped constraint space.

When $e_0 \in [0, b_0 - b_\infty)$, the constraint space formed by (6) and (7) is shown in Fig. 2. From Fig. 2, the constraint space has an approximately symmetric structure.

Where $a(t)$ and $b(t)$ serve as the upper and lower boundaries of the constraint space, respectively, and the initial range of the constraint space is $[e_0 - b_0, e_0 + a_0]$. The constraint space is similar to the traditional prescribed performance function [11,12], both exhibiting an approximately symmetric structure.

However, it is worth noting that by introducing the initial value of the tracking error e_0 in the prescribed performance function, it is ensured that the system's initial value of the tracking error falls within the constraint space. This eliminates the assumption in traditional prescribed performance control that initial value of the tracking error must lie in the constraint space.

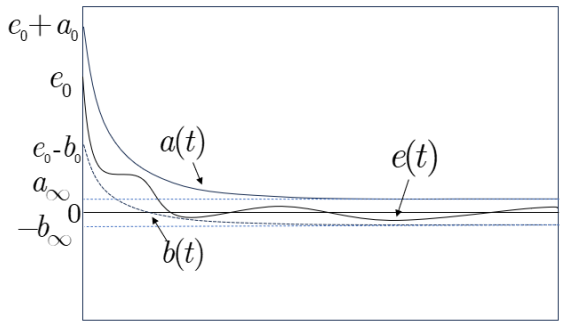

Fig. 1. Asymmetric constraints for case 1

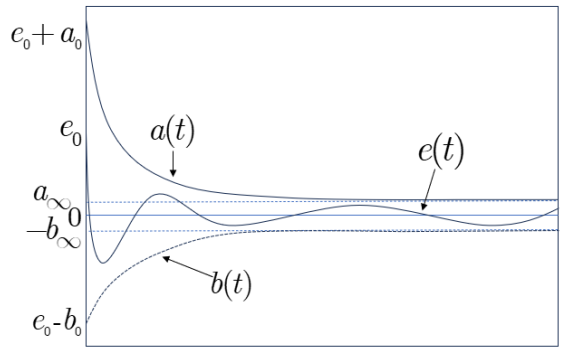

Fig. 2. Approximately symmetric constraints for case 2

Case 3: An asymmetric strip shaped constraint space

When $e_0 \in (-\infty, -(a_0 - a_\infty)]$, the constraint space formed by (6) and (7) is shown in Fig. 3. This constraint space is similar to case 1, featuring an asymmetric strip shaped constraint space, where $a(t)$ and $b(t)$ serve as the upper and lower boundaries of the constraint space, respectively. The difference lies in the initial range of the constraint space, being $[e_0 - b_0, e_0 + a_0]$ and lying on the negative half axis of y axis.

Case 4: An approximately symmetric trumpet shaped constraint space.

When $e_0 \in [-(a_0 - a_\infty), 0)$, the constraint space formed by (6) and (7) is shown in Fig. 4. This constraint space is similar to case 2, exhibiting an approximately symmetric structure. Where $a(t)$ and $b(t)$ serve as the upper and lower boundaries of the constraint space, respectively. Similarly, it ensures that the initial value of the tracking error falls within the constraint space.

Remark 1: Depending on the initial value of the tracking error e_0 and the design parameters ($a_0, a_\infty, b_0, b_\infty$), four different constraint spaces can be formed. The constraint spaces in case 2 and case 4 are approximately symmetric trumpet shaped, similar to traditional prescribed performance functions, with a larger range of variation during the initial phase. In contrast, the constraint spaces in case 1 and case 3 are asymmetric strip shaped constraint spaces with a relatively smaller variation in the initial phase, which is more conducive to reducing the fluctuations of the tracking error, decreasing the overshoot, raising transient performance.

Remark 2: Since the prescribed performance function in this paper considers the initial value of the tracking error, it ensures that the initial value of the tracking error falls within the constraint space, eliminating the assumption that initial value of the tracking error must lie in the constraint space.

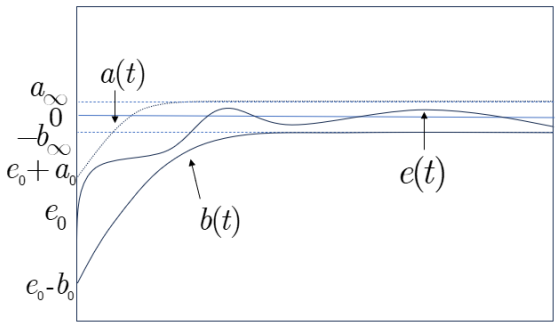

Fig. 3. Asymmetric constraints for case 3

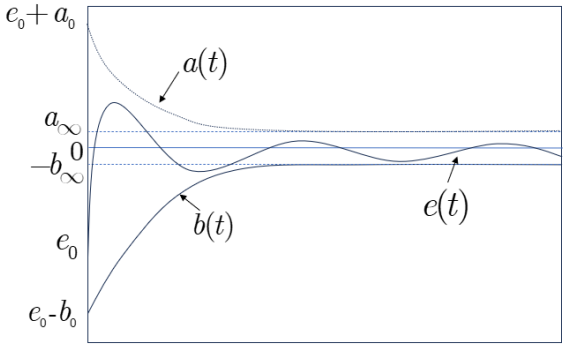

Fig. 4. Approximately symmetric constraints for case 4

Remark 3: The prescribed performance function used in this paper ensures that the system reaches a stable state within a finite time T, and the steady state error lies within the interval $(-b_\infty, a_\infty)$.

III. Controller Design

A. Prescribed Performance

Combined with the backstepping method, barrier Lyapunov function, and dynamic surface control, an asymmetric prescribed performance controller is designed for system (1) in this section.

To facilitate the use of obstacle Lyapunov functions to prove the stability of the system, the following coordinate transformation is introduced.

$$z_1(t) = 2e(t) - a(t) - b(t). \tag{8}$$

Substituting (8) into (5), we obtain

$$-\rho(t) < z_1(t) < \rho(t), \tag{9}$$

where $\rho(t) = a(t) - b(t)$, the constraints on the tracking error in (5) and (9) are equivalent. In the following, (9) will be used to design the prescribed performance controller.

The controller design process can be divided into n steps, and the following coordinate transformations are used.

$$e_i = x_i - \omega_i, \quad i = 2,\ldots,n. \tag{10}$$

where ω_i is the output of the virtual control law α_{i-1} after passing through a low pass filter, and the filtering error is defined as

$$m_i = \omega_i - \alpha_{i-1}, i = 2,\ldots,n. \tag{11}$$

The low pass filter used in this paper is shown in (12) [28].

$$\begin{cases} \tau_i \dot{\omega}_i + \omega_i = \alpha_{i-1}, \\ \omega_i(0) = \alpha_{i-1}(0), i = 2,\ldots n, \end{cases} \tag{12}$$

where α_{i-1} and ω_i are the input and output signals of the filter respectively, and $\tau_i > 0$ is design parameter.

B. Virtual Control Design

Step 1:

Taking the derivative of (8) and substituting (1), and $e_1 = y - y_r$, we obtain

$$\dot{z}_1 = 2(f_1 + g_1 x_2 - \dot{y}_r) - \dot{a} - \dot{b}. \tag{13}$$

From (6) and (7), we can obtain

$$\dot{a} = (e_0 + a_0 - a_\infty)(n+1)(1-\frac{t}{T})^n(-\frac{1}{T}), \tag{14}$$

$$\dot{b} = (e_0 - b_0 + b_\infty)(n+1)(1-\frac{t}{T})^n(-\frac{1}{T}). \tag{15}$$

Let

$$V_1 = V_{e1} + V_{m1}, \tag{16}$$

where $V_{e1} = \frac{1}{2}\ln\frac{\rho^2}{\rho^2 - z_1^2}$ and $V_{m1} = \frac{1}{2}m_2^2$.

The time derivative of V_{e1} can be written as

$$\begin{aligned}\dot{V}_{e1} &= \frac{1}{\rho^2}[\frac{\rho\dot{\rho}(\rho^2 - z_1^2) - (\rho\dot{\rho} - z_1\dot{z}_1)\rho^2}{(\rho^2 - z_1^2)}] \\ &= Q[z_1\dot{z}_1 - \frac{\dot{\rho}}{\rho}z_1^2],\end{aligned} \tag{17}$$

where $Q = 1/(\rho^2 - z_1^2)$.

Substituting (10), (11) and (13) into (17) yields

$$\begin{aligned}\dot{V}_{e1} &= Qz_1(2(f_1 + g_1\alpha_1 - \dot{y}_r) - \dot{a} - \dot{b}) \\ &\quad + 2Qz_1g_1(e_2 + m_2) - \frac{Q\dot{\rho}}{\rho}z_1^2.\end{aligned} \tag{18}$$

Based on Lemma 3, the following inequalities hold:

$$2Qg_1z_1e_2 \le Q^2g_1^2z_1^2 + e_2^2, \tag{19}$$

$$2Qg_1z_1m_2 \le Q^2g_1^2z_1^2 + m_2^2. \tag{20}$$

Substituting (19) and (20) into (18) yields

$$\begin{aligned}\dot{V}_1 &\le Qz_1(2(f_1 + g_1\alpha_1 - \dot{y}_r) - \dot{a} - \dot{b}) \\ &\quad + Qz_1(2Qz_1g_1^2 - \frac{\dot{\rho}}{\rho}z_1) + e_2^2 + m_2^2.\end{aligned} \tag{21}$$

The virtual control law is set as

$$\begin{aligned}\alpha_1 &= \frac{1}{2g_1}(-2f_1 + 2\dot{y}_r + \dot{a} + \dot{b}) \\ &\quad + \frac{1}{2g_1}(-k_1z_1 + \frac{\dot{\rho}}{\rho}z_1 - 2Qz_1g_1^2),\end{aligned} \tag{22}$$

where $k_1 > 0$ is a positive design parameter.

Substituting (22) into (21) yields

$$\dot{V}_{e1} \le -k_1Qz_1^2 + e_2^2 + m_2^2. \tag{23}$$

The time derivative of V_{m1} is

$$\dot{V}_{m1} = m_2\dot{m}_2. \tag{24}$$

From (11) and (12), through simple derivation, we can obtain

$$\dot{m}_2 = -\frac{m_2}{\tau_2} - \dot{\alpha}_1. \tag{25}$$

Substituting (25) into (24) yields

$$\dot{V}_{m1} = -\frac{m_2^2}{\tau_2} - m_2\dot{\alpha}_1. \tag{26}$$

Assume $|-\dot{\alpha}_1| \le \bar{\varsigma}_1(z_1, \dot{a}, \dot{b}, \dot{\rho}, y_r, \dot{y}_r)$, where $\bar{\varsigma}_1$ is continuous function. For simplicity, abbreviate $\bar{\varsigma}_1(z_1, \dot{a}, \dot{b}, \dot{\rho}, y_r, \dot{y}_r)$ as $\bar{\varsigma}_1$.

By Lemma 3, we can know

$$-m_2\dot{\alpha}_1 \le m_2^2 + \frac{\bar{\varsigma}_1^2}{4}. \tag{27}$$

Substituting (27) into (26), it can be obtained

$$\dot{V}_{m1} \le -\frac{m_2^2}{\tau_2} + m_2^2 + \frac{\bar{\varsigma}_1^2}{4}, \tag{28}$$

where $0 < \tau_2 < \frac{1}{2}$.

Furthermore, from (16), (23) and (28), it yields

$$\begin{aligned}\dot{V}_1 &= \dot{V}_{e1} + \dot{V}_{m1} \\ &\le -k_1Qz_1^2 - (\frac{1}{\tau_2} - 2)m_2^2 + e_2^2 + \frac{\bar{\varsigma}_1^2}{4} \\ &= -k_1\frac{z_1^2}{\rho^2 - z_1^2} - (\frac{1}{\tau_2} - 2)m_2^2 + e_2^2 + \frac{\bar{\varsigma}_1^2}{4}.\end{aligned} \tag{29}$$

By Lemma 2, (29) can be rewritten as:

$$\begin{aligned}\dot{V}_1 &\le -k_1\ln\frac{z_1^2}{\rho^2 - z_1^2} - (\frac{1}{\tau_2} - 2)m_2^2 \\ &\quad + e_2^2 + \frac{\bar{\varsigma}_1^2}{4} \\ &\le -a_1V_1 + \frac{\bar{\varsigma}_1^2}{4} + e_2^2,\end{aligned} \tag{30}$$

where $a_1 = \min\{2k_1, 2(1/\tau_2 - 1)\}$, $0 < \tau_2 < 1/2$, τ_2 is a design parameter.

Step *i*: $(2 \le i \le n-1)$

Let

$$\begin{aligned}V_i &= V_{i-1} + V_{ei} + V_{m,i+1} \\ &= V_{i-1} + \frac{1}{2}e_i^2 + \frac{1}{2}m_{i+1}^2,\end{aligned} \tag{31}$$

where

$$V_{ei} = \frac{1}{2}e_i^2, \tag{32}$$

$$V_{m,i+1} = \frac{1}{2}m_{i+1}^2. \tag{33}$$

From (1), (10), and (11), it yields

$$\dot{e}_i = f_i + g_i(e_{i+1} + m_{i+1} + \alpha_i) + \frac{m_i}{\tau_i}. \tag{34}$$

Substituting (34) for (32) yields

$$\begin{aligned}\dot{V}_{ei} &= e_i\dot{e}_i \\ &= e_i(f_i + g_ie_{i+1} + g_im_{i+1} + g_i\alpha_i + \frac{m_i}{\tau_i}).\end{aligned} \tag{35}$$

By Lemma 3, it can be inferred that

$$g_ie_ie_{i+1} \le \frac{e_i^2g_i^2}{4} + e_{i+1}^2, \tag{36}$$

$$g_i e_i m_{i+1} \le \frac{e_i^2 g_i^2}{4} + m_{i+1}^2. \tag{37}$$

Substituting (36) and (37) into (35) yields

$$\begin{aligned}\dot{V}_{ei} &\le e_i(f_i + g_i\alpha_i + \frac{m_i}{\tau_i} + \frac{g_i^2 e_i}{2}) \\ &\quad + e_{i+1}^2 + m_{i+1}^2.\end{aligned} \tag{38}$$

The virtual control law is set as

$$\alpha_i = \frac{1}{g_i}(-k_i e_i - f_i - \frac{m_i}{\tau_i} - \frac{g_i^2 e_i}{2} - e_i). \tag{39}$$

Substituting (39) into (38) yields

$$\dot{V}_{ei} \le -k_i e_i^2 - e_i^2 + e_{i+1}^2 - m_{i+1}^2, \tag{40}$$

where $k_i > 0$.

Next, we proceed to handle $V_{m,i+1}$. Taking the first derivative of (33) and assume $|-\dot{\alpha}_i| \le \bar{\varsigma}_i(e_i, m_i)$ where $\bar{\varsigma}_i(e_i, m_i)$ is continuous function. Applying the method similar to **Step 1**, it can be obtained that

$$\begin{aligned}\dot{V}_{m,i+1} &= m_{i+1}\dot{m}_{i+1} \\ &\le -\frac{m_{i+1}^2}{\tau_{i+1}} + m_{i+1}^2 + \frac{\bar{\varsigma}_i^2}{4},\end{aligned} \tag{41}$$

where $\bar{\varsigma}_i(e_i, m_i)$ is abbreviated as $\bar{\varsigma}_i$.

Taking the derivative of (31) and substituting (40) and (41)

$$\begin{aligned}\dot{V}_i &= \dot{V}_{i-1} + \dot{V}_{ei} + \dot{V}_{m,i+1} \\ &\le -a_{i-1}V_{i-1} - k_i e_i^2 - (\tfrac{1}{\tau_{i+1}} - 2)m_{i+1}^2 \\ &\quad + \sum_{j=1}^{i} \frac{\bar{\varsigma}_j^2}{4} + e_{i+1}^2 \\ &\le -a_i V_i + \sum_{j=1}^{i} \frac{\bar{\varsigma}_j^2}{4} + e_{i+1}^2,\end{aligned} \tag{42}$$

where $a_i = \min\{a_{i-1}, 2k_i, 2(1/\tau_{i+1} - 2)\}$, $0 < \tau_{i+1} < 1/2$ is a design parameter.

Step *n*:

Let

$$V_n = V_{n-1} + \frac{1}{2}e_n^2. \tag{43}$$

By taking the first derivative of (43), it yields

$$\dot{V}_n = \dot{V}_{n-1} + e_n\dot{e}_n. \tag{44}$$

From (1), (10), and (11), we obtain

$$\dot{e}_n = f_n + g_n u + \frac{m_n}{\tau_n}. \tag{45}$$

Substituting (45) for (44) yields

$$\dot{V}_n = \dot{V}_{n-1} + e_n(f_n + g_n u + \frac{m_n}{\tau_n}). \tag{46}$$

The actual control law is set as

$$u = \frac{1}{g_n}(-k_n e_n - f_n - \frac{m_n}{\tau_n} - e_n). \tag{47}$$

Substituting (43) and (47) into (46) yields

$$\begin{aligned}\dot{V}_n &\le -a_{n-1}V_{n-1} - k_n e_n + \sum_{i=1}^{n-1} \frac{\bar{\varsigma}_i^2}{4} \\ &\le -a_{\min}V_n + b,\end{aligned} \tag{48}$$

where $a_{\min} = \min\{a_{n-1}, 2k_n\}$, $b = \sum_{i=1}^{n-1} \frac{\bar{\varsigma}_i^2}{4}$.

From Lemma 1, the following theorem can be derived.

Theorem 1: Under the condition that assumption 1 is satisfied, when the virtual control laws are given by (22) and (39), and the actual control law is given by (47), by appropriately selecting $k_i > 0\ (i = 1,2,\cdots,n)$ and $0 < \tau_{i+1} < 1/2$ $(i = 1,2,\cdots,n-1)$, the closed loop system (1) is uniformly ultimately bounded stable at the origin. Furthermore, the system satisfies the performance requirements predefined by (5).

IV. SIMULATION RESULTS

To justify the effectiveness of the asymmetric prescribed performance controller designed in this paper, the following second order system is selected:

$$\begin{cases}\dot{x}_1 = f_1 + g_1 x_2, \\ \dot{x}_2 = f_2 + g_2 u,\end{cases} \tag{49}$$

where $f_1 = x_1^2 + 1$, $f_2 = x_2^2 + 1$, $g_1 = x_1^2 + 1$, $g_2 = x_2^2 + 1$, $y_r = \sin(At) + A\cos(0.5At)$, and $A = 1$.

A. Performance Simulation Analysis of Asymmetric Prescribed Performance Control

To demonstrate the impact of the initial value of the tracking error and the parameters of the prescribed performance function on the controller, simulations are conducted for the four possible cases mentioned earlier. The specific details are as follows:

Case 1: $e_0 \in [b_0 - b_\infty, \infty)$,

Case 2: $e_0 \in [0, b_0 - b_\infty)$,

Case 3: $e_0 \in (-\infty, -(a_0 - a_\infty)]$,

Case 4: $e_0 \in [-(a_0 - a_\infty), 0)$.

The initial value of the tracking error for case 1 and case 2 are greater than 0 $(e_0 \ge 0)$, while the initial value of the tracking error for case 3 and case 4 are less than 0 $(e_0 < 0)$. The simulation duration is set to 6s, with design parameters, $k_1 = k_2 = 10$, the filter parameter $\tau_{12} = 0.2$, and initial value of the filter $\omega_1(0) = 3$. Other parameters required for the simulation are listed in Table I. The simulation time is uniformly set to 6s.

TABLE I
PARAMETER SETTING

Type of Situation	Parameter Settings
Case 1	$e_0 = 2$, $b_0 = 0.5$, $b_\infty = 0.08$, $a_0 = 3$, $a_\infty = 0.08$.
Case 2	$e_0 = 0.2$, $b_0 = 3$, $b_\infty = 0.08$, $a_0 = 3$, $a_\infty = 0.08$.
Case 3	$e_0 = -4$, $a_0 = 3$, $a_\infty = 0.08$, $b_0 = 0.5$, $b_\infty = 0.08$.
Case 4	$e_0 = -2$, $a_0 = 3$, $a_\infty = 0.08$, $b_0 = 0.5$, $b_\infty = 0.08$.

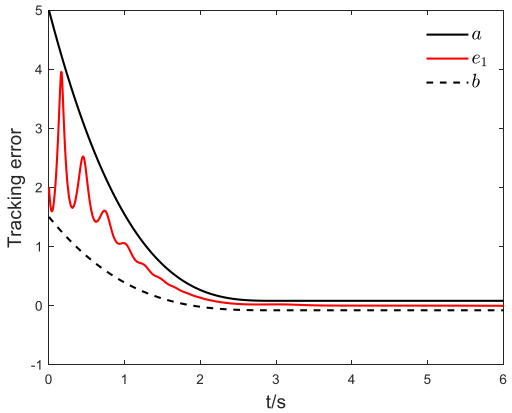

(a) Simulation of case 1: asymmetric constraints.

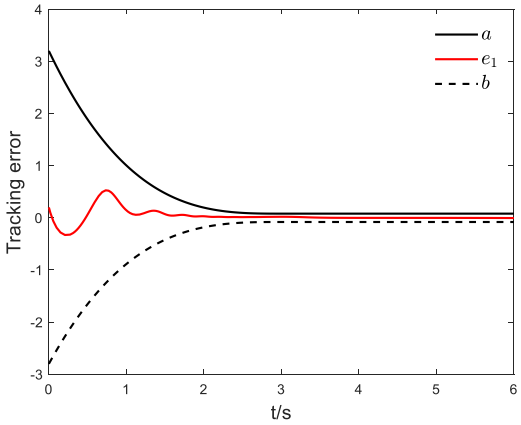

(b) Simulation of case 2: approximately symmetric constraints.

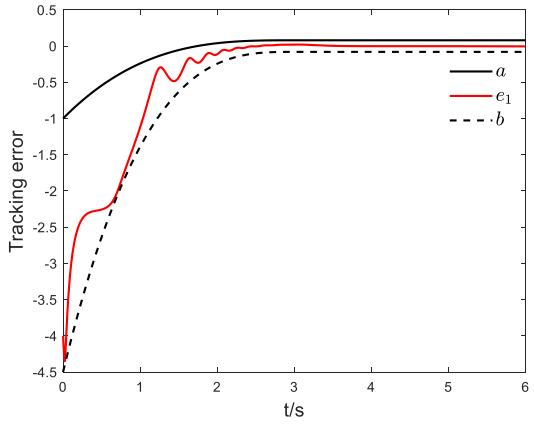

(c) Simulation of case 3: asymmetric constraints.

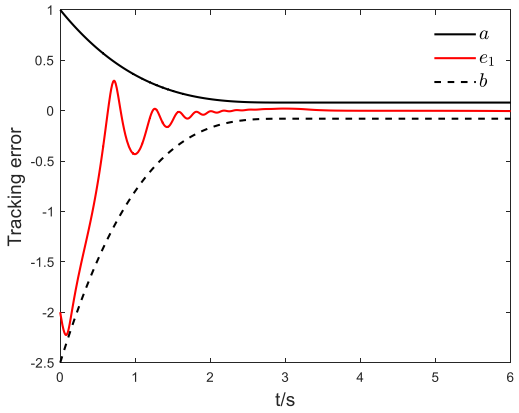

(d) Simulation of case 4: approximately symmetric constraints.

Fig. 5. Constraint curves of the APPC

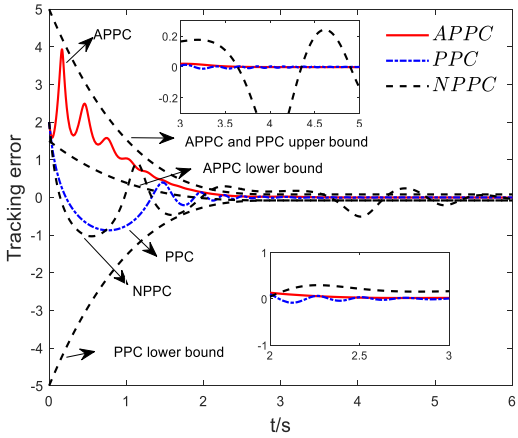

Fig. 6. Tracking error.

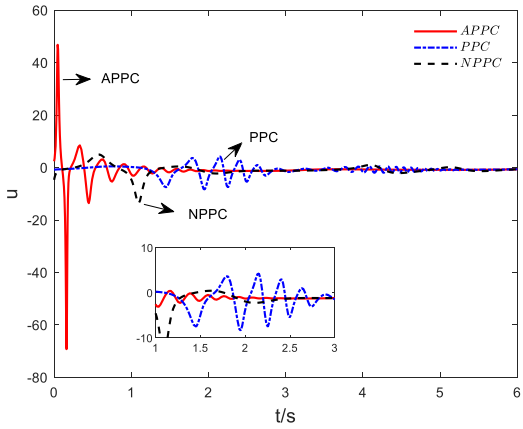

Fig. 7. Output signals of the controllers.

The variation curve of system tracking error $e_1(t)$ over time is shown in Fig. 5. For clarity, both the upper bound a and lower bound b of the asymmetric prescribed performance function are provided in the simulation. As shown in Fig. 5, the controller designed in this paper has achieved good control effects, ensuring that the tracking error of the system converges quickly and remains within the constraint range formed by the prescribed performance function.

From Fig. 5, when different control parameters are selected, the prescribed performance function can form four different types of constraint spaces: the asymmetric strip shaped constraint space shown in Fig. 5(a) and Fig. 5(c), and the approximately symmetric trumpet shaped constraint space shown in Fig. 5(b) and Fig. 5(d).

The range of the strip shaped constraint space is significantly smaller than that of the trumpet shaped constraint space. Therefore, with approximately the same settling time, the strip shaped constraint space has a smaller constraint range and the tracking error changes more smoothly.

B. Comparison with Traditional Prescribed Performance Control

To justify the effectiveness of the asked algorithm, simulations were also conducted for the prescribed performance controller (PPC) [11, 12] and the finite time controller without prescribed performance (NPPC) [29], the model was adopted by (49).

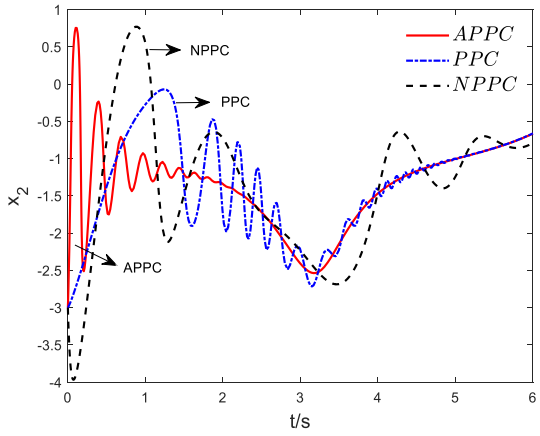

Fig. 8. State variable x_2.

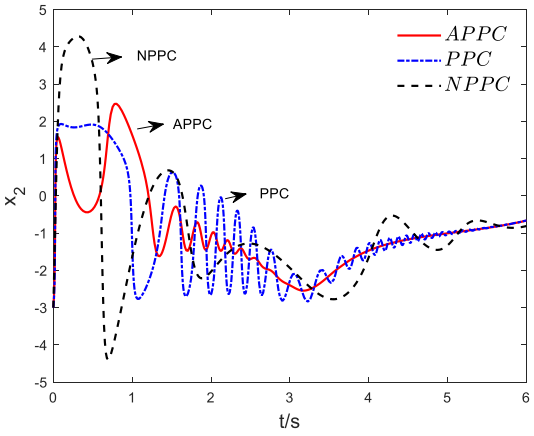

Fig. 11. Time varying curves of the state variable x_2.

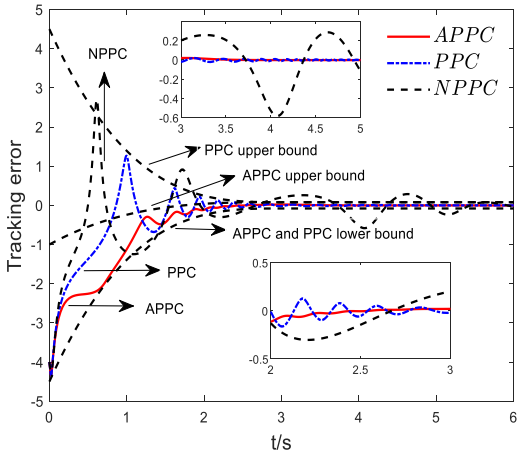

Fig. 9. Time varying curves of the tracking error.

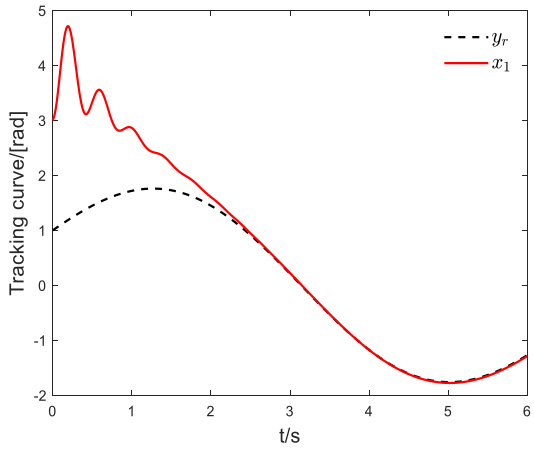

Fig. 12. Tracking curve.

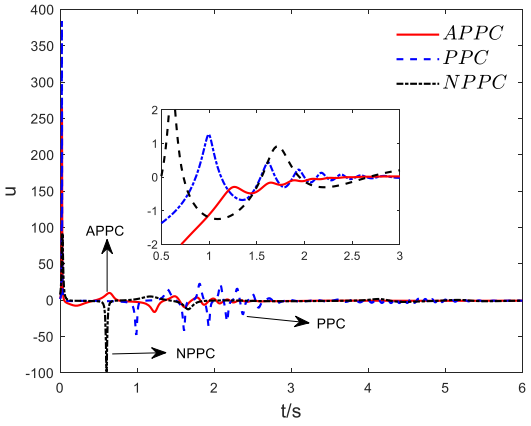

Fig. 10. Output signals of the controllers.

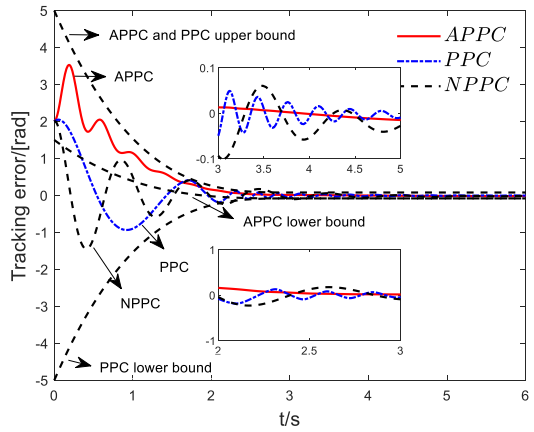

Fig. 13. Tracking error.

Both cases where the initial value of the tracking error was greater than 0 and less than 0 were considered. To verify the performance of the proposed APPC controller when the initial value of the tracking error is greater than 0, the initial states of system are chosen as $x_1(0)=3$, $x_2(0)=-3$, the initial tracking error is 2. Other parameters used in the simulation are listed in Table II. Fig. 6 shows the time varying curves of the tracking error. For clarity, the upper and lower bounds of the constraint spaces for both APPC and PPC are also provided in Fig. 6, where *a, b* and $-a$ represents the bound of the constraint space for both APPC and PPC, respectively.

TABLE II
SIMULATION PARAMERTES

Algorithm	Constraint Parameters	Filter Parameters	Scale Factor
APPC	$a_0=3$, $a_\infty=0.08$, $b_0=0.5$, $b_\infty=0.08$.	$\omega_{12}=-3$, $\tau_{12}=0.2$.	$k_1=5$, $k_2=5$.
PPC	$a_0=3$, $a_\infty=0.08$.	$\omega_{22}=-3$, $\tau_{22}=0.5$.	$c_1=5$, $c_2=5$.
NPPC	/	$\omega_{32}=-3$, $\tau_{32}=0.5$.	$K_1=5$, $K_2=5$.

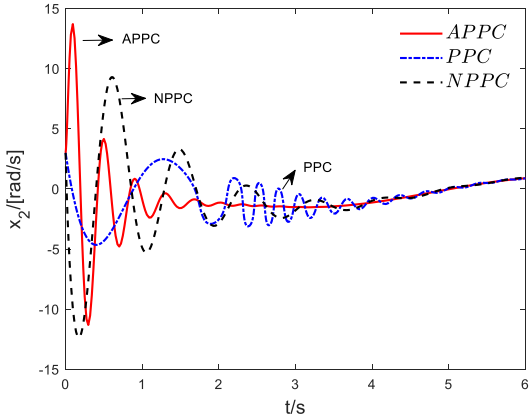

Fig. 14. State variable x_2.

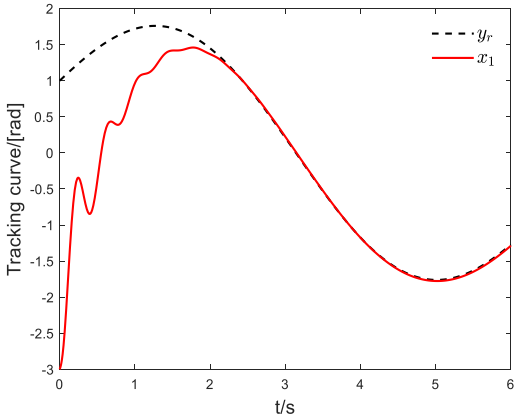

Fig. 16. Tracking curve.

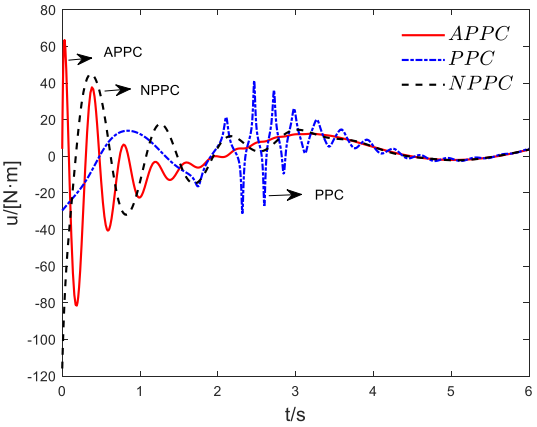

Fig. 15. Output signals of controllers.

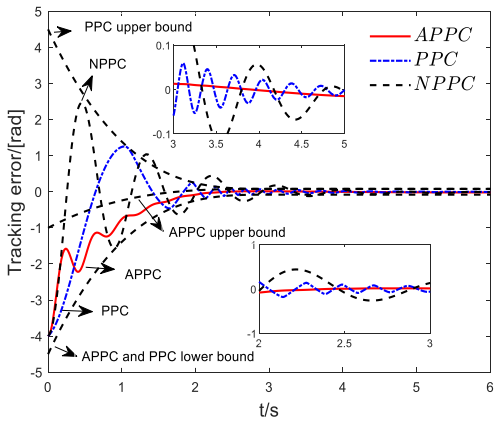

Fig. 17. Tracking error.

Both the APPC and PPC controllers exhibit significantly lower settling times and overshoot compared to the NPPC controller. This is primarily because the prescribed performance control in APPC and PPC predefines the convergence speed and variation range of the tracking error, thereby improving the transient performance.

Compared to the PPC controller, the APPC controller not only has a smaller settling time and overshoot but also exhibits smaller fluctuations in transient process. This is mainly due to the predefined asymmetric strip shaped constraint space imposing stronger constraints on the tracking error, further enhancing the transient performance. Fig. 7 shows the output variation curves of the three aforementioned controllers.

From Fig. 7, the APPC control signal exhibits fast convergence speed, with particularly small fluctuations in the later stage. Time varying curves of the state variable x_2 for the three controllers mentioned above are shown in Fig. 8. It can be seen that the state variable x_2 is bounded and physically realizable.

To verify the effectiveness of the proposed APPC controller when the initial value of the tracking error is less than 0, the initial states of system are chosen as $x(0)=[x_1(0), x_2(0)]^T=\left[-3,-3\right]$ with the initial tracking error being -4. Other parameters are the same as those in Table II. Fig. 9 shows the error tracking curves for the APPC, PPC, and NPPC controllers. Fig. 10 presents the output signals of the three controllers mentioned above. Fig. 11 displays the time varying curves of the state variable x_2.

Fig. 9-11, conclusions like those in the previous section can be drawn, the APPC exhibits the smallest fluctuations and overshoot in transient process, demonstrating the best transient performance. It ensures that the closed loop system tracking error remains within the predefined asymmetric strip shaped constraint space and converges to a small neighborhood near the origin within the finite time T.

V. PRACTICAL APPLICATION

To verify the effectiveness of the proposed method, the designed controller is applied to the rigid robotic arm system described in [30], whose dynamic model as follows:

$$\begin{cases}\dot{x}_1 = x_2,\\ \dot{x}_2 = f_2 + g_2 u,\end{cases} \tag{50}$$

where x_1, x_2 and u are the angular position, angular velocity and input torque of the robotic arm respectively, $f_2=-m_r g_v l_r \cos(x_1)/J_0$, $g_2=1/J_0$, inertial coefficient $J_0=4m_r l_r^2/3$, load mass $m_r=5kg$, gravitational acceleration $g_v=9.8m/s^2$, length of the robotic arm $l_r=0.25m$.

A. *The Initial Value of Tracking Error Is Greater Than* 0

We first consider the case where the initial error is greater than 0. Let $x_1(0)=3$, $x_2(0)=3$, and the initial tracking error is 2. The other parameters in the simulation are shown in Table III. The simulation time is uniformly set to 6s.

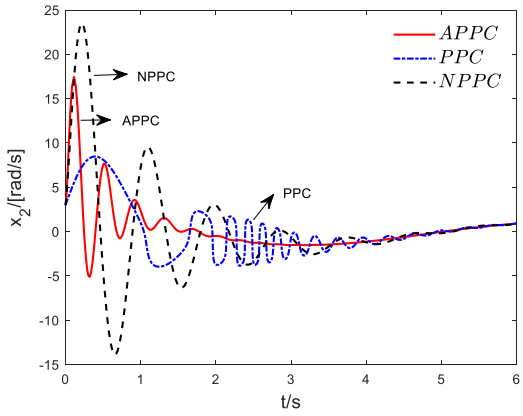

Fig. 18. Time varying curves of the state variable x_2.

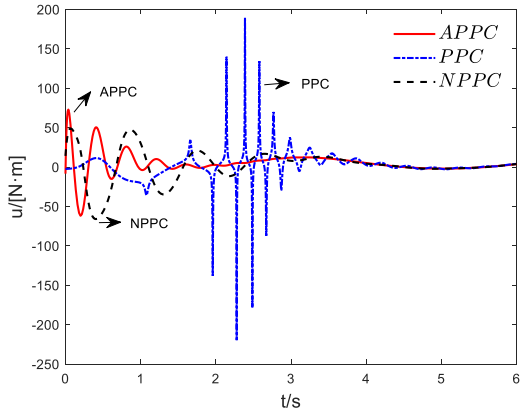

Fig. 19. Output signals of controllers.

The simulation results are shown in Fig. 12 to Fig. 15. Fig. 12 displays the tracking trajectory of the robotic arm system, while Fig. 13 illustrates the corresponding tracking error curves. Key observations from Fig. 13 include: All three controllers (APPC, PPC, and NPPC) successfully drive the tracking error to converge within a small neighborhood of the origin. The APPC controller demonstrates superior transient performance, exhibiting minimal oscillation (zero overshoot) and the fastest convergence (settling time of 2.02s), significantly outperforming both the PPC controller (1.02rad overshoot, 2.86s settling time) and NPPC controller (1.56rad overshoot, 3.02s settling time). Regarding steady-state error, the APPC controller (0.02rad) shows 23% and 38% improvement over the PPC (0.026rad) and NPPC (0.032rad) controllers respectively. This performance advantage can be attributed to the asymmetric prescribed performance function employed in the APPC controller, which features more precise constraint space and finite-time convergence properties. Fig. 14 shows the curves of the robotic arm's angular velocity x_2. As can be seen from Fig. 14, the state x_2 is bounded. Fig. 15 presents the curves of the control input u. From Fig. 15, it is evident that the control signal meets practical requirements. The analysis shows that the APPC algorithm proposed in the paper has obvious advantages over the traditional PPC algorithm.

B. The Initial Value of Tracking Error Is Less Than 0

We consider the case where the initial error is less than 0 in this section. Let $x_1(0) = -3$, $x_2(0) = 3$, the initial value of the tracking error is selected as -4. Other parameters are the same as those in Table III. The simulation time is uniformly set to 6s.

TABLE III
SIMULATION PARAMERTES

Algorithm	Constraint Parameters	Filter Parameters	Scale Factor
APPC	$a_0 = 3$, $a_\infty = 0.08$. $b_0 = 0.5$, $b_\infty = 0.08$.	$\omega_{12} = -3$, $\tau_{12} = 0.2$.	$k_1 = 100$, $k_2 = 100$.
PPC	$a_0 = 3$, $a_\infty = 0.08$.	$\omega_{22} = -3$, $\tau_{22} = 0.5$.	$c_1 = 12$, $c_2 = 8$.
NPPC	/	$\omega_{32} = -3$, $\tau_{32} = 0.5$.	$K_1 = 50$, $K_2 = 50$.

The simulation results are shown in Fig. 16 to Fig. 19, Fig. 16 presents tracking curve of the robotic arm system. Fig. 17 presents tracking error curves, Fig. 18 shows the curves of the robotic arm's angular velocity x_2, and Fig. 19 presents the curves of the control input u.

Similar conclusions to the previous section can be drawn from Fig. 16-Fig. 19. The APPC controller has not only excellent transient characteristics but also excellent steady state characteristics. In the transient process, APPC controller has the smallest fluctuation and no overshoot. APPC controller and PPC controller have almost the same setting time, but both are significantly smaller than that of NPPC. After entering the steady state process, the fluctuation of APPC control is also smaller than PPC controller and NPPC controller.

VI. CONSIDERATION

The paper investigates the issue of asymmetric prescribed performance constraints for a class of strict feedback nonlinear systems. A finite time prescribed performance function with an asymmetric structure in a strip shaped constraint space is proposed, and a controller is designed based on this prescribed performance function to address the issue of large tracking error fluctuations caused by the expansive constraint space of traditional prescribed performance controllers. By treating the initial value of the tracking error as a parameter of the prescribed performance function, the paper ensures that the initial value of the tracking error can fall within the constraint range, thereby broadening the applicability of prescribed performance control. The designed controller guarantees that the tracking error of the strict feedback nonlinear system converges to a small neighborhood near the coordinate origin in finite time, and all signals in the closed loop system are bounded. Simulation results validate the effectiveness of the proposed control scheme. Future research will further explore and paper the integration of sliding mode control in [31, 32]. The sliding mode control has strong robustness, and the sliding mode control is further combined with the prescribed performance control to improve the system ability to resist interference, and is applied to more complex industrial application contexts.

REFERENCES

[1] C. K. Gong, Q. Y. Ru, and L. P. Yuan, "Adaptive Constraint Control of Unknown Strict Feedback Nonlinear Systems under Dead Zone Input," *Applied Mathematics and Mechanics*, vol. 43, no. 12, pp. 1402-1411, 2022.

[2] Y. B. Zang, N. N. Zhao, X. Y. Ouyang, and J. N. Zhao, "Prescribed Performance Adaptive Control for Nonlinear Systems with Unmodeled Dynamics Via Event-triggered," *Engineering Letters*, vol. 31, no. 4, pp. 1770-1779, 2023.
[3] Y. B. Jiang, Z. X. Liu, and Z. Q. Chen, "Distributed Fault-tolerant Consensus Tracking Control for Multiple Lagrangian Systems with Preset Error Bound Constraints," *Journal of the Franklin Institute*, vol. 358, no. 14, pp. 6994-7012, 2021.
[4] J. Wu, W. Wang, and J. Li, "Adaptive Optimized Fuzzy Control of Uncertain Strict Feedback Systems with Preset Tracking Accuracy," *International Journal of Fuzzy Systems*, vol. 25, no. 7, pp. 2699-2711, 2023.
[5] Y. S. Hu, H. C. Yan, M. Wang, Y. F. Chang, and K. B. Shi, "Practical Preset Time Fault-tolerant Control of Uncertain Euler-Lagrange Systems with Input Saturation and Guaranteed Performance," *International Journal of Robust and Nonlinear Control*, vol. 34, no. 5, pp. 3259-3277, 2024.
[6] D. D. Mu, J. S. Li, G. F. Wang, and Y. S. Fan, "Research on Path Following Control of Unmanned Ship Based on Fast Wave Inversion Disturbance Compensation and Prescribed Performance," *Ocean Engineering*, vol. 304, no. 17864, pp. 1-14, 2024.
[7] Y. N. Yang, Y. W. Yan, C. C. Hua, J. P. Li, and K. L. Pang, "Prescribed Performance Control for Teleoperation System of Nonholonomic Constrained Mobile Manipulator Without Any Approximation Function," *IEEE Transactions on Automation Science and Engineering*, vol. 21, no. 3, pp. 2900-2911, 2023.
[8] X. Li, J. Qian, D. N. Tian, Y. Zeng, F. Gao, and *et al*., "Maximum Power Tracking Control of Wind Turbines Based on a New Prescribed Performance Function," *Energies*, vol. 16, no.10, pp. 1-21, 2023.
[9] D. G. Chu, and Y. Liu, "Adaptive Neural Network Control with Quantified Input for Robotic Arm System with Prescribed Performance," *Electronic Technology,* vol. 37, no. 12, pp. 1-7, 2024.
[10] Y. L. Huang, and H. J. Li, "Prescribed Performance Control of Intelligent Vehicle Steering System Based on RBFNN," *Journal of Liaoning University of Engineering and Technology (Natural Science Edition)*, vol. 43, no. 01, pp. 85-92, 2024.
[11] K. X. Lu, H. Q. Wang, F. Zheng, and W. Bai, "Finite-time Prescribed Performance Tracking Control for Nonlinear Time-delay Systems with State Constraints and Actuator Hysteresis," *ISA Transactions*, vol. 153, no. 1, pp. 295–305, 2024.
[12] X. N. Xia, Z. L. Yin, C. Li, X. L. Zhang, and S. Wu, "Finite Time Dynamic Surface Control of Nonlinear Systems with Input Delay and Prescribed Performance," *Journal of Jiangsu University (Natural Science Edition)*, vol. 45, no. 03, pp. 316-322, 2024.
[13] G. Q. Duan, and G. P. Liu, "Adaptive Prescribed Performance Control of Combined Spacecraft Pose Based on Full Drive System Method," *Chinese Journal of Aeronautics*, vol. 45, no. 01, pp. 127-136, 2024.
[14] X. L. Zhang, Y. Zhang, Q. Hu, X. Guo, Y. X. Yang, and *et al*., "Model-free Based Fixed-time Control for The Uncertain Wearable Exoskeleton with Preset Performance," *Control Engineering Practice*, vol. 151, no. 106011, pp. 1-11, 2024.
[15] S. H. Gao, X. P. Liu, Y. W. Jing, and Georgi M. Dimirovski, "A Novel Finite-time Prescribed Performance Control Scheme for Spacecraft Attitude Tracking," *Aerospace Science and Technology*, vol. 118, no. 107044118, pp. 1-15, 2021.
[16] F. Liu, and M. Chen, "Fuzzy Adaptive Control of Turbofan Engine Under Fixed Time Prescribed Performance," *Chinese Science: Information Science*, vol. 54, no. 07, pp. 1793-1806, 2024.
[17] L. P. Xin, B. Yu, L. Zhao, and J. P. Yu, "Adaptive Fuzzy Backstepping Control for a Two Continuous Stirred Tank Reactors Process Based on Dynamic Surface Control Approach," *Applied Mathematics and Computation*, vol. 377, no. 01, pp. 125-138, 2020.
[18] G. Luo, P. X. Li, and Z. L. Feng, and B, X. Ma, "Event-triggered Steering Control for Automated Vehicles with Prescribed Performance," *IEEE Access*, vol. 9, no. 01, pp. 104560-104571, 2021.
[19] A. Q. Wang, J. L. Li, G. F. Xia, and H. J. Chen, "Four Rotor Unmanned Aerial Vehicle Prescribed Performance Adaptive PID Control," *Control Engineering*, vol. 31, no. 05, pp. 865-875, 2024.
[20] H. X. Ma, M. Chen, and Q. X. Wu, "Prescribed Performance Safety Tracking Control of Unmanned Helicopters with Input and output Constraints," *Control Theory and Application*, vol. 41, no. 01, pp. 39-48, 2024.
[21] Z. Y. Gao, Z. C. Sun, and G. Guo, "Fixed Time Global Prescribed Performance Vehicle Queue Control Considering Actuator Nonlinearity," *Journal of Automation*, vol. 50, no. 2, pp. 320-333, 2024.
[22] Y. Cheng, B. Cheng, H. D. Du, and L. Xu, "Design of Guided Missile Control System Based on Dynamic Surface Control," *Journal of Weapon Equipment Engineering*, vol. 45, no. 8, pp. 135-139+167, 2024.
[23] Z. B. Xu, C. Gao, and H. Z. Jiang, "High-Gain-Observer-Based Output Feedback Adaptive Controller Design with Command Filter and Event-triggered Strategy," *IAENG International Journal of Applied Mathematics*, vol. 53, no. 2, pp. 463-469, 2023.
[24] Q. M. Cheng, Z. C. Shen, L. Zhang, H. L. Wang, W. T. Wang, and *et al*., "Lyapunov Function Control Strategy for Hexagonal Converter for Low frequency Offshore Wind Power," *Southern Power Grid Technology*, vol. 06, no. 25, 06, pp. 1-13, 2024.
[25] Y. C. Huang, J. H. Wang, F. Wang, and B. T. He, "Event-triggered Adaptive Finite-time Tracking Control for Full State Constraints Nonlinear Systems with Parameter Uncertainties and Given Transient Performance," *ISA Transactions*, vol. 108, no. 1, pp. 131-143, 2021.
[26] X. H. Li, H. Q. Bao, and H. Liu. "Finite Time Bounded H_∞ Control for Prescribed Performance of Nonlinear Systems with Unknown Initial Tracking Conditions," *Control and Decision*, vol. 39, no. 07, pp. 2215-2223, 2024.
[27] Y. A. Hu, B. L. Geng, and Y. T. Zhao, "Design of Backstepping Controller with Strict Feedback on Prescribed Performance of Nonlinear Systems," *Control and Decision*, vol. 29, no. 08, pp. 1509-1512, 2014.
[28] Y. S. Li, M. Chen, H. Q. Wang, and K. X. Peng, "Finite Time Adaptive Dynamic Facial Error Control for Nonlinear Systems," *Control Theory and Application*, vol. 39, no. 08, pp. 1489-1496, 2022.
[29] J. Li, J. T. Qiu, H. T. Gao, "Design and Application of Dynamic Surface Active Disturbance Rejection Controller for Nonlinear Systems," *Journal of Harbin Engineering University*, vol. 38, no. 08, pp. 1278-1284, 2017.
[30] X. P. Liu, H. Q. Wang, C. Gao, and M. Chen, "Adaptive Fuzzy Funnel Control for a Class of Strict Feedback Nonlinear Systems," *Neurocomputing*, vol, 241, no. 01, pp. 71-80, 2017.
[31] R. Chen, Z. You, and W. Zhang, "Adaptive Fuzzy Sliding Mode Control for Nonlinear Systems with Unknown Dead-zone," *IAENG International Journal of Applied Mathematics*, vol. 54, no.12, pp. 2588-2595, 2024.
[32] E. Giraldo, "Adaptive Dead-beat Sliding Plane Multivariable Decoupled Control of a Microgrid," *IAENG International Journal of Applied Mathematics*, vol. 52, no. 4, pp. 1070-1079, 2022.

Xinen Liu, born in Chaoyang, Liaoning, China, August 1994, is a Ph.D. student in the class of 2022 in the School of Electronic and Information Engineering, University of Science and Technology Liaoning (USTL), and received the B.S. degree in Automation from USTL in 2017 and the M.S. degree in Control Science and Engineering from USTL in 2020, Anshan, Liaoning, China. His research interests are nonlinear control theory research, intelligent control.

He is currently a lecturer in the School of Electrical and Automation Engineering, Liaoning Institute of Science and Technology, Benxi, Liaoning, China.